(12) LEVEL II

FINAL REPORT

of

Contract F49620-79-C-0168

16 May 1979 - 31 December 1979

THREE-DIMENSIONAL TRANSIENT NATURAL CONVECTION IN A HORIZONTAL CYLINDER: A NUMERICAL ANALYSIS

See 1473 in back.

by

JAMES A LIBURDY
Principal Investigator

CLEMSON UNIVERSITY
MECHANICAL ENGINEERING DEPARTMENT
CLEMSON, SOUTH CAROLINA 29631

for the

AIR FORCE OFFICE OF SCIENTIFIC RESEARCH
DIRECTORATE OF AEROSPACE SCIENCES
BOLLING AFB, DC 20332

Approved for public release; distribution unlimited.

February 1980

UNCLASSIFIED

THREE DIMENSIONAL TRANSIENT NATURAL CONVECTION IN A HORIZONTAL CYLINDER: A NUMERICAL ANALYSIS

SUMMARY

This final report discusses work completed under USAF Office of Scientific Research Contract F49620-79-C-0168 under the technical guidance of Dr. D. G. Samaras in the period 16 May 1979 through 31 December 1979.

A mathematical formulation of the governing equations for transient natural convection in a finite length horizontal cylinder are developed and constructed in finite difference form. The boundary conditions consist of radial heat flux for a specified thermal resistance, axial heat flux from one closed end and three different conditions at the other end to represent exposure to a hot convecting gas environment. The formulation is expressed in terms of the vorticity equations, energy equation and a set of vector potential equations. Solution is by the ADI (alternating direction implicite) method for the vorticity and energy equations and the SOR (successive overrelation) method for the vector potential equations.

Numerical experiments were run using the model to determine the local wall heat flux and the local wall temperatures. Wall thermal resistance values and the aspect ratio (length-to-diameter) was chosen to be consistant with the Air Force test facility at Arnold Air Station. A heat transfer correlation is presented in terms of the Nusselt and Rayleigh numbers. Steady state conditions are obtained for the nondimensional time $(\frac{t\nu}{r_o^2})$ approximately equal to .005. Circumferential heat transfer coefficient variations are shown with larger values occurring near the top of the

cylinder. Axial coefficients vary within approximately ±10% with the largest values occurring near the center of the cylinder. With respect to test conditions at the Arnold Air Station facility, the convective components appear to be less than 10% of the radiative heat flux to the cylinder walls when a high temperature gas (air) is enclosed in the cylinder.

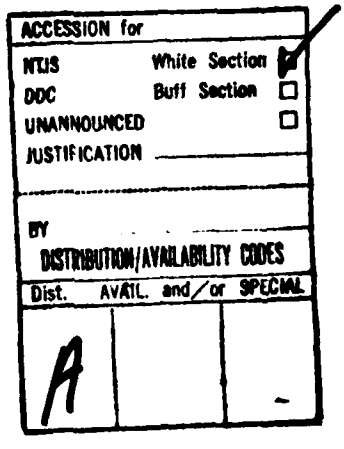

ACKNOWLEDGMENTS

This research was supported by the United States Air Force Office of Scientific Research, Contract No. F49620-79-C-0168. The work was performed under the technical management of Dr. Demetrious G. Samaras of the Aerospace Science branch.

TABLE OF CONTENTS

	Page
Summary	i
Acknowledgments	iii
Table of Contents	iv
Nomenclature	v
Research Objectives	1
Status of Research Objectives	2
Mathematical Model	2
Numerical Procedure	7
Results	14
Recommendations for Further Studies	25
Publications and Paper Presentations	27
Associated Personnel	28
References	29

NOMENCLATURE

A - representative nondimensional dependent variable, Equation (6)

B - term in finite difference approximation, Equation (6)

C - constant, Equation (6)

c_p - specific heat at constant pressure

F - nondimensional function of the independent variable

g - acceleration due to gravity, directed down

G - Grashoff number = $g\beta(2r_o)^3 T_o/\nu^2$

G_r - Grashoff number = $G\Delta T/T_o$

h - convective film coefficient

i,j,k- subscripts in the finite difference approximations

k - thermal conductivity

L - length of cylinder

n - time step

Nu - Nusselts number = $\frac{h(2r)}{k}$

Pr - Prandtl number = ν/α

q - heat flux at a solid surface

Qi - nondimensional temperature gradient at a solid surface

r - radial coordinate

r_o - cylinder radius

R - nondimensional radial coordinate = r/ro

Ra - Rayleigh number = Pr Gr

S - representative nondimensional dependent variable, Equation (11)

t - time variable

T - temperature

T_o - initial temperature

ΔT - prescribed temperature difference

U - ϕ velocity component

V - r velocity component

$\bar{V}$ - nondimensional velocity vector

w - z velocity component

Z - axial distance

Greek Letters

β - thermal expansion coefficient

δ - differential operator

θ - nondimensional temperature

ν - viscosity

τ - nondimensional time

ϕ - circumferential component

$\bar{\psi}$ - vector potential

ω - nondimensional vorticity

RESEARCH OBJECTIVES

The specific research objectives of this study are as follows:

(i) Develop a model of three-dimensional transient natural convection in a horizontal cylinder with one closed end and one open end which is subjected to various conditions of temperature and velocity.

(ii) Perform numerical calculations on this model to obtain velocity and temperature distributions.

(iii) Integrate the foregoing model with an existing radiation model to predict the inside surface temperature of the cylinder.

STATUS OF RESEARCH OBJECTIVES

Mathematic Model

The research objectives numerated previously have been completed. An analytical tool for examining an enclosed transient three-dimensional cylincrical natural convection flow field has been developed. The impetus for this investigation developed from the need to predict internal temperature distributions of high temperature gas containment vessels used by the U.S. Air Force in engine test facilities. A schematic of this type of facility is shown in Figure 1. The natural convective heat flux influence on the wall temperature history appears to be approximately 10% of the radiative component. The test facility was modelled using a right horizontal cylinder lined with insulating refractor brick, closed at one end and open at the other end. The coordinate system used is shown in Figure 2. The open end is in direct contact with hot gases and has been modelled under various assumptions discussed later. An aspect ratio (length-to-diameter) of 3.15 was used in all numerical experiments.

The governing equations for the conservation of mass, momentum and energy are recast in terms of the vorticity transport equation, and the energy equation with a defining equation for the vector potential. A similar formulation was used by Aziz and Hellums [1] for cartesian coordinates. In vector notation the system of equations becomes:

$$\frac{D\omega}{D\tau} = \bar{\omega} \cdot \nabla\bar{V} + \nabla^2\bar{\omega} - Gr \begin{bmatrix} -\frac{\partial\theta}{\partial z}\cos\phi \\ -\frac{\partial\theta}{\partial z}\sin\phi \\ \frac{\partial\theta}{\partial R}\sin\phi + \frac{1}{R}\frac{\partial\theta}{\partial\phi}\cos\phi \end{bmatrix} \qquad (1)$$

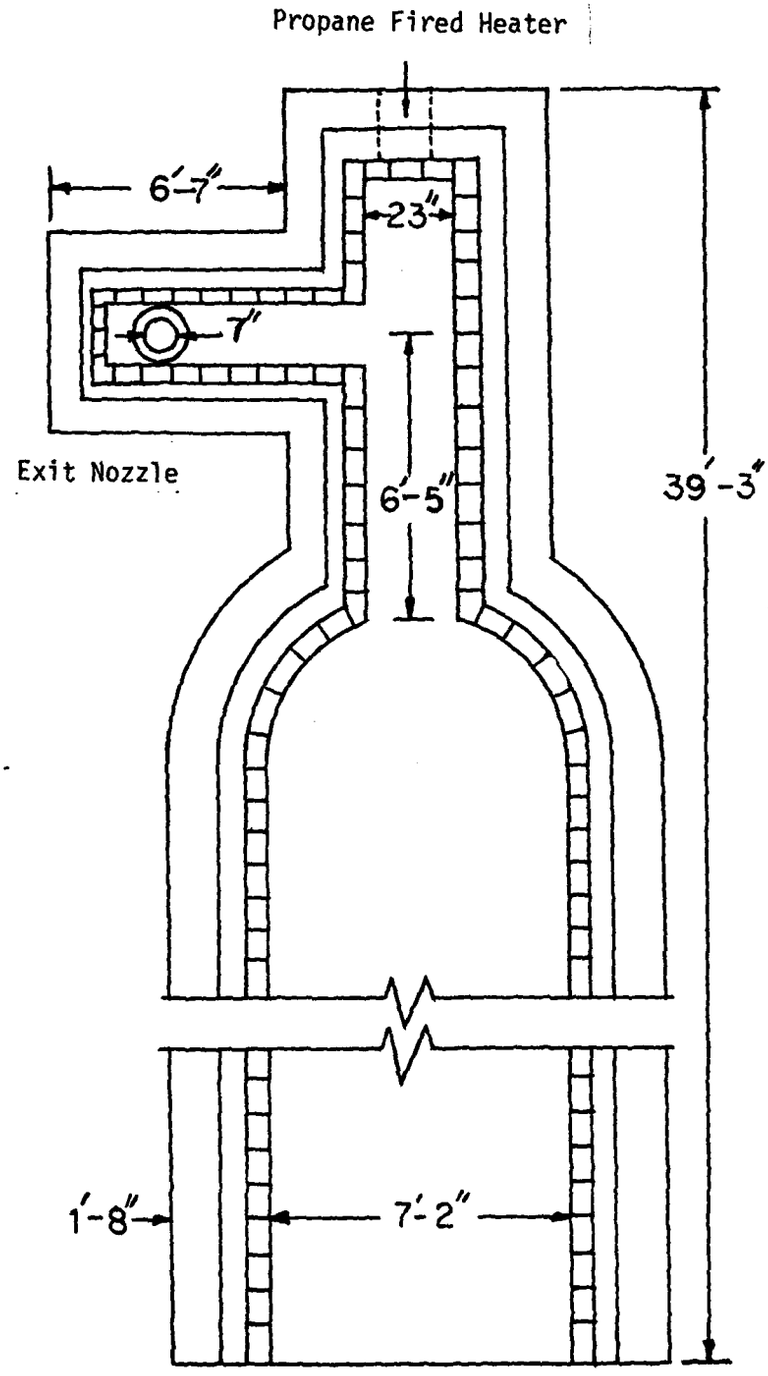

Figure 1. Schematic of the high temperature gas heater used in U.S.A.F. engine test facility at Arnold Air Station, TN.

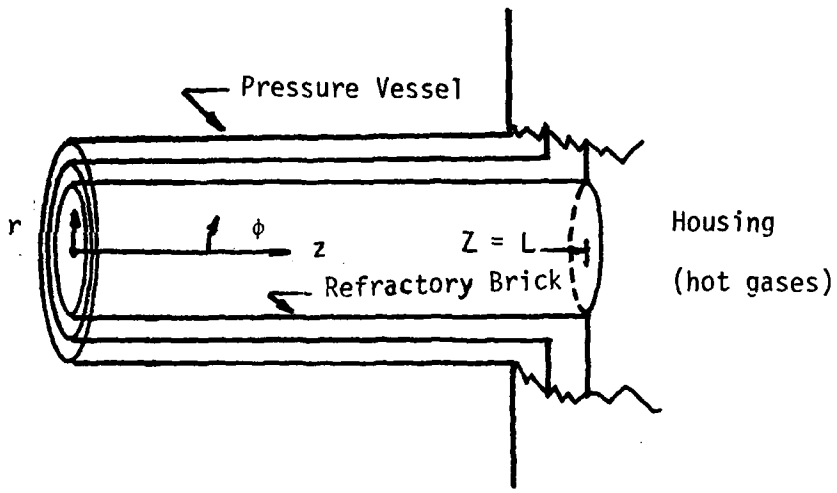

Figure 2. Geometry and coordinate system of the horizontal extension arm of the high temperature gas heater.

$$\frac{D\theta}{D\tau} = \frac{1}{Pr} \nabla^2\theta \tag{2}$$

where the vorticity is defined by:

$$\nabla \times \bar{V} = \bar{\omega} \tag{3}$$

such that

$$\nabla^2\bar{\psi} = -w \tag{4}$$

and the vector potential is defined by the relationship

$$\bar{V} = -\nabla \times \bar{\psi} \tag{5}$$

The variables used in the above equations have been nondimensionalized with respect to the time scale (r_o^2/ν), and length scale r_o.

This mathematical formulation is based on the following assumptions applied to the fluid system:

(i) Newtonian behavior with constant viscosity and thermal conductivity

(ii) the Boussinesq approximation where the density variations are only introduced into the body force terms in the momentum equations

(iii) negligible viscous dissipation in the energy equation

(iv) a linear density-temperature relationship with a coefficient of thermal expansion β

(v) negligible coriolis and centrifugal forces in the ϕ and r momentum equations respectively.

The boundary conditions are as follows. At the periphery and the closed end of the cylinder a thermal resistance is specified based on the wall composite thermal resistivity and an external convective resistance based on empirical correlation of heat transfer from horizontal cylinders (see McAdams [2]). An arbitrary ambient temperature was chosen. Since the open end is exposed to hot gases which will also be under the influence of convective heat transfer, various boundary conditions were explored.

The conditions chosen were:

(i) a constant uniform temperature and zero velocity to represent a uniform static environment

(ii) a linear temperature profile in the vertical direction and zero velocity to represent a stratified, static environment

(iii) a linear temperature profile as in (ii) but with a constant finite velocity to represent a convecting downward flow,

In case (i) the constant temperature was chosen as the initial hot temperature of the gas. The linear temperature profiles of cases (ii) and (iii) were ±20°F about the assumed initial starting temperature. The relative effects of each of these conditions will be discussed later.

The boundary conditions, expressed in terms of the nondimensional variables defined in the Nomenclature are:

$R = 1$: $\omega_R = 0$

$$\omega_\phi = \frac{\partial W}{\partial R}$$

$$\omega_Z = -\frac{\partial u}{\partial R}$$

$$\frac{\partial \theta}{\partial R} = Q_1$$

$Z = 0$: $\omega_R = \frac{\partial U}{\partial Z}$

$$\omega_\phi = -\frac{\partial v}{\partial Z}$$

$$\omega_z = 0$$

$$\frac{\partial \theta}{\partial z} = Q_2$$

$$Z = L: \qquad (1) \quad \omega_R = \frac{\partial U}{\partial Z}$$

$$\omega_\phi = -\frac{\partial V}{\partial Z}$$

$$\omega_z = 0 \qquad \text{(STAGNANT-STRATIFIED)}$$

$$\theta = F_1(R,\phi,Z)$$

$$(2) \quad \tilde{\omega} = F_2(R,\phi,Z) \quad \text{(CONVECTIVE-STRATIFIED) CONDITION}$$

$$\theta = F_3(R,\phi,Z)$$

where the functions F_1, and F_3 represents the assumed nondimensional temperature profiles, and F_2 is the curl of the assumed velocity profile at $Z = L$.

Numerical Procedure

The numerical modelling scheme used to solve the system of Equations (1) - (5) was a modified version of that used by Aziz and Hellums [1] for a rectangular enclosure. The grid arrangement is shown in Figure 3.a. In order to evaluate the dependent variables at the centerline, a Cartesian coordinate system was imposed along the line $r = 0$ as indicated in Figure 3.b. This eliminates the differencing equations from blowing up along this line and was found to be more accurate than using the limiting form of the differential equations at $r = 0$ (see Kee and McKillop [3]).

The numerical procedure consists of three stages per time step. First the parabolic equations are solved for $A^{(1)}$ which represents a first

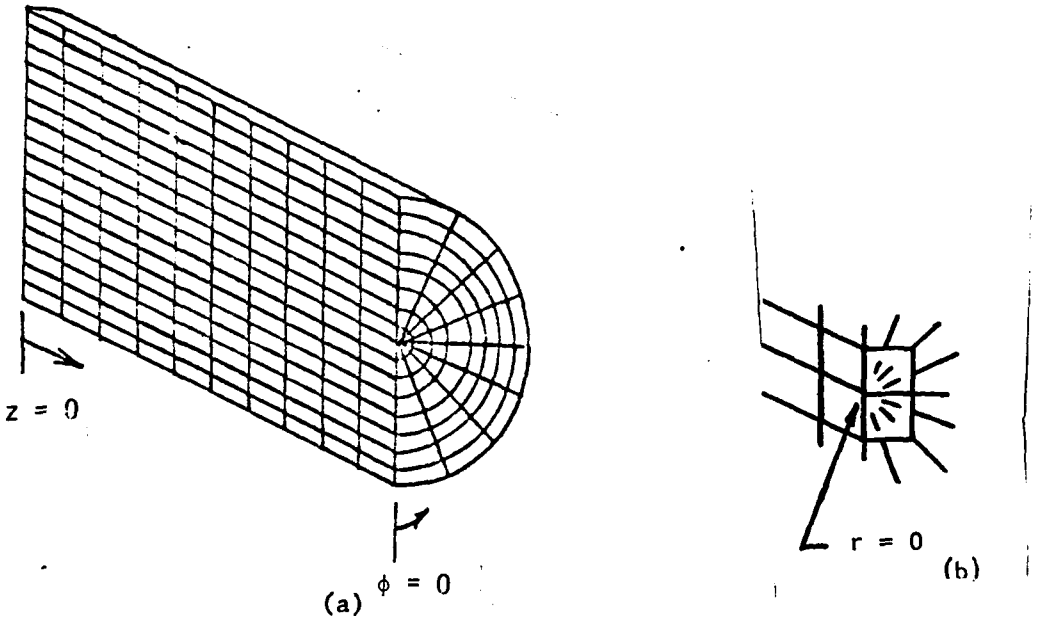

Figure 3. (a) Grid system for the finite difference approximation
(b) Blow-up of the grid about r = 0.

approximation of the dependent variable due to changes in the ϕ direction at a given time step, then a second approximation, $A^{(2)}$, at the same time step due to changes in the r direction is obtained, and lastly $A^{(3)}$ is calculated based on changes in the z direction. The system of equations solved is:

$$\frac{A_{n+1}^{(1)} - A_n^{(0)}}{\Delta\tau} = C\left[\tfrac{1}{2}\,\delta_\phi\left(A_{n+1}^{(1)} + A_n^{(0)}\right) + \delta_R\left(A_n^{(0)}\right) + \delta_Z\left(A_n^{(0)}\right) + B\right]$$

$$\frac{A_{n+1}^{(2)} - A_n^{(0)}}{\Delta\tau} = C\left[\tfrac{1}{2}\,\delta_\phi\left(A_{n+1}^{(1)} + A_n^{(0)}\right) + \tfrac{1}{2}\,\delta_R\left(A_{n+1}^{(2)} + A_n^{(0)}\right) + \delta_Z\left(A_n^{(0)}\right) + B\right] \tag{6}$$

$$\frac{A_{n+1}^{(3)} - A_n^{(0)}}{\Delta\tau} = C\left[\tfrac{1}{2}\,\delta_\phi\left(A_{n+1}^{(1)} + A_n^{(0)}\right) + \tfrac{1}{2}\,\delta_R\left(A_{n+1}^{(2)} + A_n^{(0)}\right) + \tfrac{1}{2}\,\delta_Z\left(A_{n+1}^{(3)} + A_n^{(0)}\right) + B\right]$$

In the above expressions C represents a constant and equals one when solving for the vorticity components and 1/Pr in evaluating the temperatures. The delta functions, δ, represent the following combinations of first and second derivatives:

$$\delta_\phi = \frac{1}{R}\,\frac{\partial^2}{\partial\phi^2} - \frac{U}{R}\,\frac{\partial}{\partial\phi}$$

$$\delta_R = \frac{\partial^2}{\partial R^2} - \left(V - \frac{1}{R}\right)\frac{\partial}{\partial R} \tag{7}$$

$$\delta_Z = \frac{\partial^2}{\partial Z^2} - W\,\frac{\partial}{\partial Z}$$

The conventional symmetric finite difference forms for the first and second derivatives were used to evaluate each δ to assure errors of the order of the grid size squared. As an illustration of how Equations (6) were applied consider the following formulation to evaluate the first approximation of ω_ϕ, the ϕ component of the vorticity at an interior node (i,j,k):

$$\frac{\overset{(1)}{\omega_\phi}_{n+1}(i,j,k) - \overset{(0)}{\omega_\phi}_{n}(i,j,k)}{\Delta\tau} = \tfrac{1}{2}\left\{\left(\frac{\overset{(1)}{\omega_\phi}(i+1,j,k) - 2\overset{(1)}{\omega_\phi}(i,j,k)+\overset{(1)}{\omega_\phi}(i-1,j,k)}{R^2\Delta\phi^2} - \frac{U(i,j,k)}{R}\left(\frac{\overset{(1)}{\omega_\phi}(i+1,j,k) - \overset{(1)}{\omega_\phi}(i-1,j,k)}{2\Delta\phi}\right)\right)_{n+1}\right.$$

$$+ \left(\frac{\overset{(0)}{\omega_\phi}(i+1,j,k) - 2\overset{(0)}{\omega_\phi}(i,j,k) + \overset{(0)}{\omega_\phi}(i-1,j,k)}{R^2\Delta\phi^2} - \frac{U(i,j,k)}{R}\cdot\right.$$

$$\left.\left.\frac{\overset{(0)}{\omega_\phi}(i+1,j,k) - \overset{(0)}{\omega_\phi}(i-1,j,k)}{2\Delta\phi}\right)_{n}\right.$$

$$+ \left(\frac{\overset{(0)}{\omega_R}(i,j+1,k) - 2\overset{(0)}{\omega_R}(i,j,k) + \overset{(0)}{\omega_R}(i,j,-1,k)}{\Delta R^2} - \frac{RV(i,j,k)-1}{R}\cdot\right.$$

$$\left.\left.\frac{\overset{(0)}{\omega_R}(i,j,+1,k) - \overset{(0)}{\omega_R}(i,j-1,k)}{2\Delta R}\right)_{n}\right.$$

$$+ \left(\frac{\overset{(0)}{\omega_Z}(i,j,k+1) - 2\overset{(0)}{\omega_Z}(i,j,k) + \overset{(0)}{\omega_Z}(i,j,k-1)}{\Delta Z^2} - W(i,j,k)\cdot\right.$$

$$\left.\left.\left.\frac{\overset{(0)}{\omega_Z}(i,j,k+1) - \overset{(0)}{\omega_Z}(i,j,k-1)}{2\Delta Z}\right)_{n}\right\}\right.$$

$$+ \left[-G \frac{\partial \theta}{\partial Z} \cos\phi + \frac{2}{R^2} \frac{\partial \omega R}{\partial \phi} \frac{\omega_\phi^{(0)}}{R^2} - \frac{U(i,j,k)\omega_R^{(0)}(i,j,k)}{R} + \frac{\omega_\phi^{(0)}}{R} \frac{\partial U}{\partial \phi} + \right.$$

$$\left. \omega_R \frac{\partial U}{\partial R} + \omega_Z^{(0)} \frac{\partial U}{\partial R} + \frac{V(i,j,k)\ \omega_R}{R} \right]_n \qquad (8)$$

The term in square brackets represents the B term in Equations (6). Similar equations result for ω_R, ω_Z and θ, (the dimensionless temperature). Once the above equation is solved for $\omega_{\phi_{n+1}}^{(1)}$ it is stored and the equation for $\omega_{\phi_{n+1}}^{(2)}(i,j,k)$ is solved using $\omega_{\phi_{n+1}}^{(1)}$ in the δ_ϕ operator as indicated in Equations (8).

It is desirable to keep the error of the order of the grid size squared. As such the following approximations for the derivatives at the boundary were used:

$$\left(\frac{\partial A}{\partial R}\right)_{R=1} = \frac{1}{2(\Delta R)} \Big\{ 3A(i,j,k) - 4A(i,j-1,k) + A(i,j-2,k) \Big\}$$

$$\left(\frac{\partial^2 A}{\partial R^2}\right)_{R=1} = \frac{1}{(\Delta R)^2} \Big\{ -2A(i,j,k) + 5A(i,j-1,k) - 4A(i,j-2,k) +$$

$$A(i,j-3,k) \Big\} \qquad (9)$$

with similar expressions for the derivatives in the Z direction at the closed end.

In order to assure the least error introduced in the finite difference approximation of the time derivatives it is necessary that B and the velocity components be evaluated at $n + \frac{1}{2}$ or $n + 1$. This requires a two stage iteration scheme. First the vorticity and temperature are evaluated using

the old values of B from which the vector potential and velocity components are calculated (this procedure is outlined further on and requires an iteration procedure). These updated values are then reinserted into the parabolic set of equations to reevaluate ω and θ at the same time step. New values of $\overline{\Psi}$ and $\overline{V}$ are then calculated and again used to update ω and θ. This is continued until a predetermined convergence criteria is satisfied (that is, the fractional change in the updated and old values is less than some tolerance). Once completed the entire process is repeated at the next time step.

There is the further requirement to specify the vorticity at the solid boundaries, R=1 and Z=0. These are obtained indirectly by examining the boundary conditions for the vector potential. Morean (see Reference [1]) concludes that the normal derivatives of the normal $\overline{\Psi}$ component at a solid surface is identically zero. Further, the tangential component of $\overline{\Psi}$ to the surface also must vanish to satisfy the no-slip conditions. Transforming these conditions into the vorticity components yields the following:

$$
\begin{aligned}
R = 1: \quad \omega_\phi &= \frac{\partial W}{\partial R} = \frac{1}{2(\Delta R)} \left(4W(i\ k-1,k) - W(i,j-2,k)\right) \\
\omega_R &= 0 \\
\omega_Z &= -\frac{\partial U}{\partial R} = \frac{-1}{2(\Delta R)} \left(4U(i,j-1,k) - U(i\ k-2,k)\right) \\
Z = 0: \quad \omega_\phi &= -\frac{\partial V}{\partial Z} = \frac{1}{2(\Delta Z)} \left(4V(i,j,k+1) - V(i,j,k+2)\right) \\
\omega_R &= \frac{\partial U}{\partial R} = \frac{-1}{2(\Delta Z)} \left(4U(i,j,k+1) - U(i,j,k+2)\right) \\
\omega_Z &= 0
\end{aligned}
\tag{10}
$$

where the finite difference approximations are second-order in the space coordinates. This formulation implies that new, or updated, values of the velocity components are required to evaluate updated vorticity components at the boundaries.

The solution scheme for the elliptic equations for $\overline{\Psi}$ is as follows. A successive overrelaxation method is used to solve the finite difference approximation which can be expressed in the following form:

$$S_n^{(m)}(i,j,k) = \frac{\omega_{opt}}{\Delta_p}\left[\frac{S_n^{(m-1)}(i,j,k+1) + S_n^{(m)}(i,j,k-1)}{\Delta Z^2} + \frac{S_n^{(m-1)}(i,j+1,k) + S_n^{(m)}(i,j-1,k)}{\Delta R^2} + \frac{S_n^{(m)}(i,j+1,k) - S_n^{(m)}(i,j-1,k)}{2R\Delta R} + \frac{S_n^{(m-1)}(i+1,j,k) + S_n^{(m)}(i-1,j,k)}{R^2\Delta\phi^2} - \Delta_p S_n^{(m-1)}(i,j,k)\right] - \omega_{opt}\,\S + S_n^{(m-1)}(i,j,k) \quad (11)$$

where Δ_p is dependent on the grid size and is defined in the nomenclature. The superscripts (m) and (m-1) represent current and previous iteration values respectively. The term § is the appropriate component of vorticity to correspond with the particular vector potential component being evaluated. In this expression ω_{opt} represents an acceleration parameter and can take on values typically in the range zero to two. An optimal value was found which is designed to provide the fastest rate of convergence. (See Forsythe

and Wason [4].)

Equation (10) is iterated upon until the fractional change in the vector potential component is less than some set tolerance. The convergence is tested at each nodal location in order to assure that the entire system is well behaved. This was later changed to a selected representative point to shorten the computational time.

The grid spacing was 9 x 9 x 11. That is, the radial increment equals $r_o/8$, the angle increment $\pi/8$ and the longitudinal increment L/(10). Later a 9 x 9 x 6 grid system proved to be effective.

The program was run until steady state conditions were obtained. Steady state is determined by evaluating the total heat loss rate from the cylinder. When the heat loss rate no longer varies within one percent, steady state is assumed.

A flow chart for the solution algorithm is shown in Figure 4.

Results

The numerical experiments run to date are here summarized. The solid boundary thermal resistance was calculated using a three layer composite wall consisting of refractory brick, an insulating wall and a pressure vessel. Values of the thermal properties were obtained from an existing test facility at Arnold Air Station, TN. Variation of these values by ±20% did not alter the results presented herein. The relatively low conductivity wall of the system results in rather quickly established steady-state. However, the wall was assumed to be in local equilibrium with the instantaneous gas state which would tend to reduce the transient times

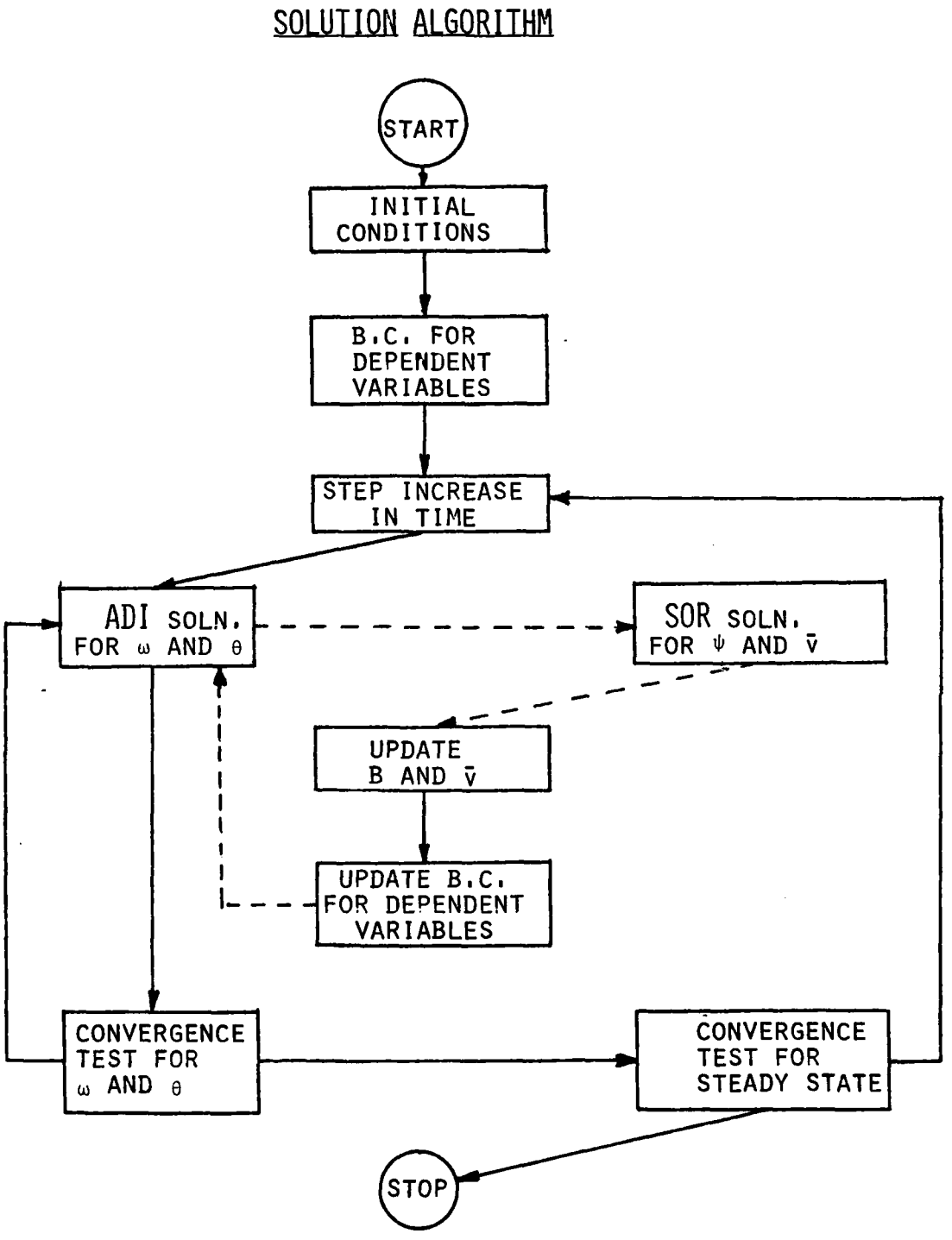

Figure 4. Solution Algorithm for the finite difference solution of the transient convection problem.

somewhat. This effect was not rigorously studied in this investigation, but an examination of the wall thermal capacitance shows that it should be a minor effect.

The majority of the results are presented in terms of the nondimensional convective film coefficient - the Nusselts number, Nu defined as

$$\overline{Nu} = \frac{\overline{h}(2r_o)}{k}$$

$$\text{where } \overline{h} = \frac{q''_{wall}}{(\overline{T}_b - \overline{T}_w)}$$

$\overline{T}_b$ = average bulk temperature of the fluid

$\overline{T}_w$ = average wall temperature.

Local values of Nu were also found at each point on the wall. Average values at each axial location were calculated based on the radial plane average bulk temperature and wall temperature. The wall heat flux was determined at each point from the local wall temperature gradient using a three point approximation for the finite difference representation.

The transient nature of the wall heat flux is best shown in the Nu vs. nondimensional time plot of Figure 5. These results are for the open end boundary condition case (i) but all three cases essentially yield the same results. Steady state conditions occur when $\tau \geq .005$. The experimental results of Evans and Stefany [5] for transient convection in a horizontal cylinder with a step change in wall temperature indicate steady values of the film coefficient, h, after approximately 20 seconds using n-butanal. Evaluating the thermal properties of n-butanal at the average fluid temperature used by Evans and Stefany in their 2.5 inch diameter cylinder results

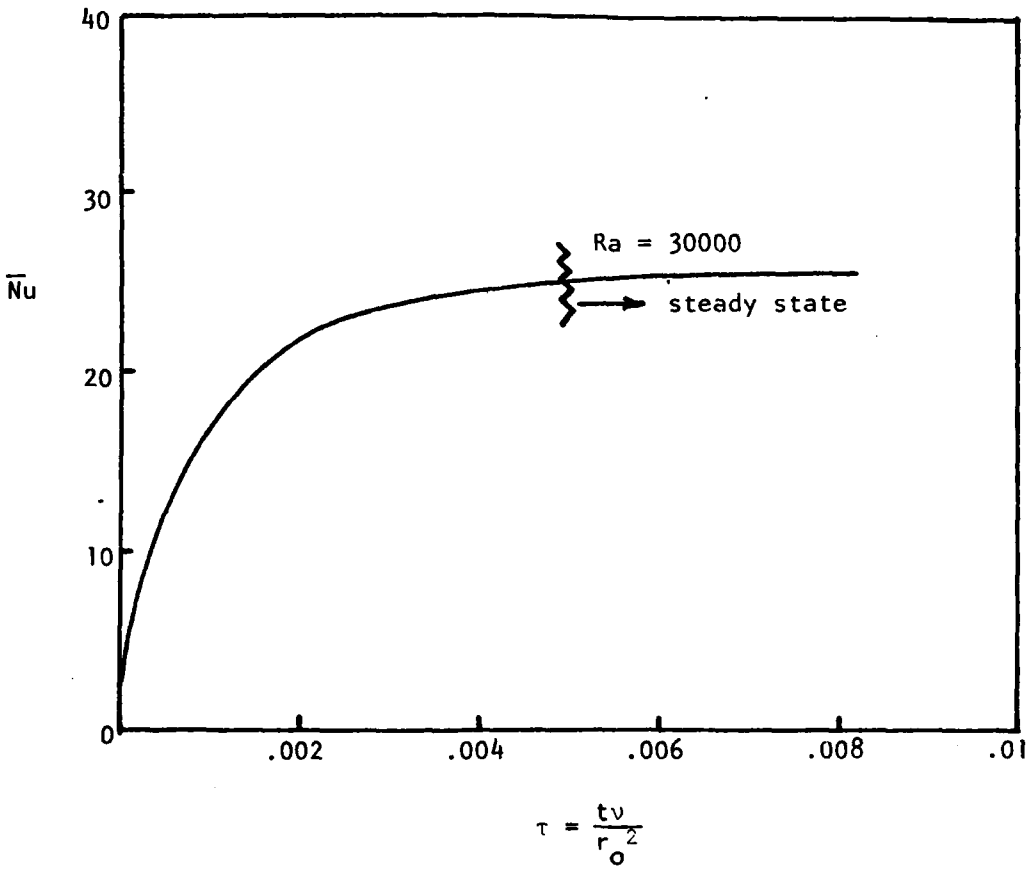

Figure 5. Transient nature of $\overline{Nu}$ versus nondimensional time, steady state reach at $\tau \approx .005$.

in a value of $\tau = .0048$ which is in agreement with these numerical results.

The boundary condition imposed, of uniform wall cooling results in cooler fluid near the boundary than in the central region. The cooler fluid sinks and sets up a clockwise convection current. This motion is depicted in Figure 6. Typical isotherms and two dimensional vector potentials (stream lines) are shown as functions of time. An upwardly buoyed motion is seen by the mushroomed shaped isotherms. The vortex type motion has a sinking center of rotation with increasing time.

The induced motion results in only slight variations of the local Nu around the cylinder. Figure 7 shows the increased heat transfer rates near the top of the cylinder.

Axial variations in local values of Nu are shown in Figure 8 for all three cases studied. At Z=0 the solid boundary impedes the convective motion resulting in lower values of Nu. At the open boundary, Z=L, only slightly higher values of Nu result for case (iii) compared to (i) and (ii) where case (iii) is the imposed constant velocity and linear temperature gradient. Removing the velocity but retaining the temperature gradient also slightly increases the radial heat transfer from the cylinder. In addition, the axial location of maximum heat transfer is shifted back towards the closed end. A rough schematic of the axial isotherm and vector potential lines are shown in Figure 9 for case (i). A hot central core exists with temperature gradients toward the conducting surfaces. Two longitudinal convection cells exist (for the range of Ra investigated).

A correlation of the $\overline{Nu}$ vs. Ra was calculated for the geometric and boundary condition constraints imposed. The Rayleigh number is defined in terms of the temperature difference $(\overline{T}_b - \overline{T}_w)$ and fluid properties were

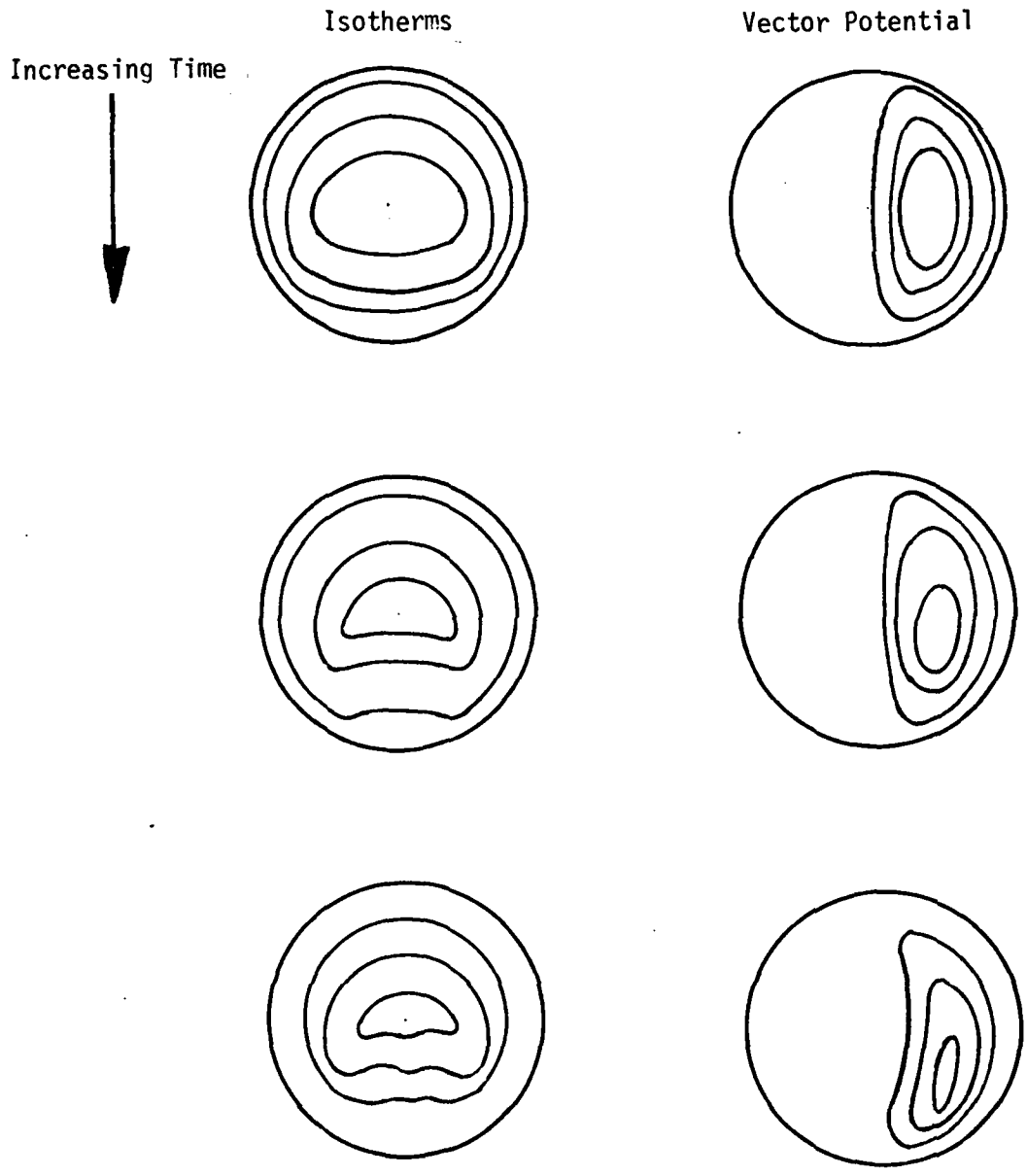

Figure 6. Representative isotherm and vector potential variation with time in the r,ϕ plane.

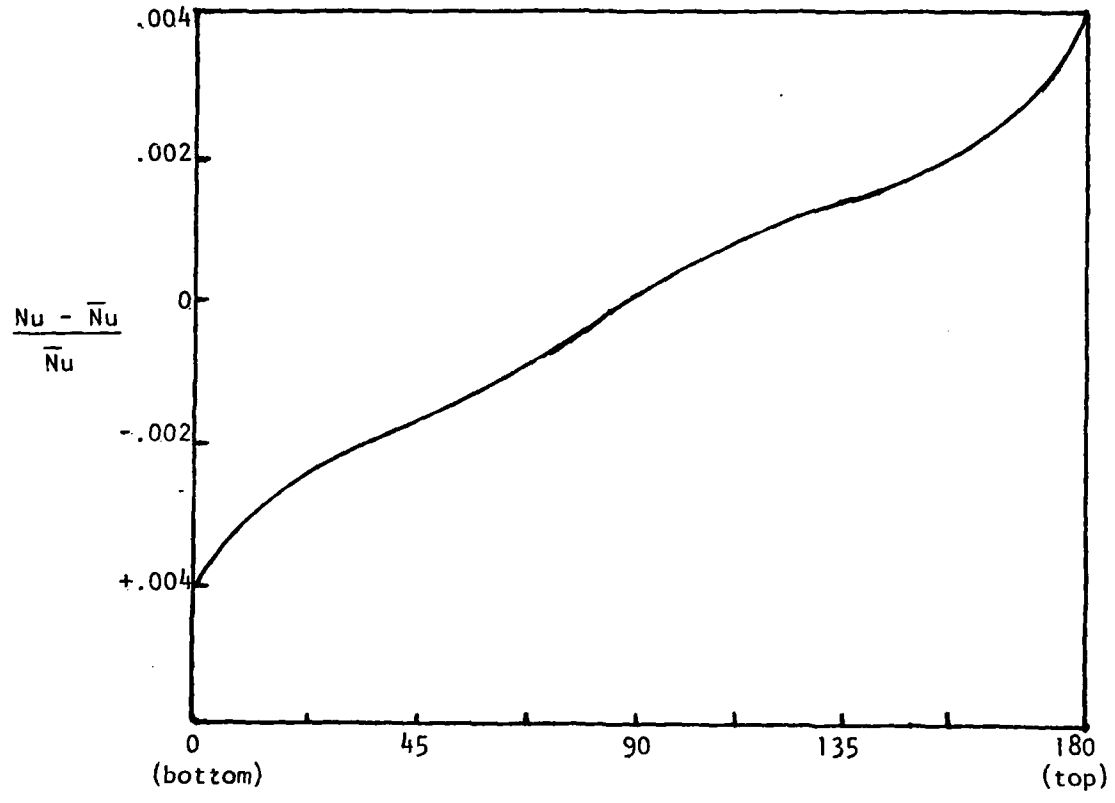

Figure 7. Circumferential variation of the local Nusselt number at steady state.

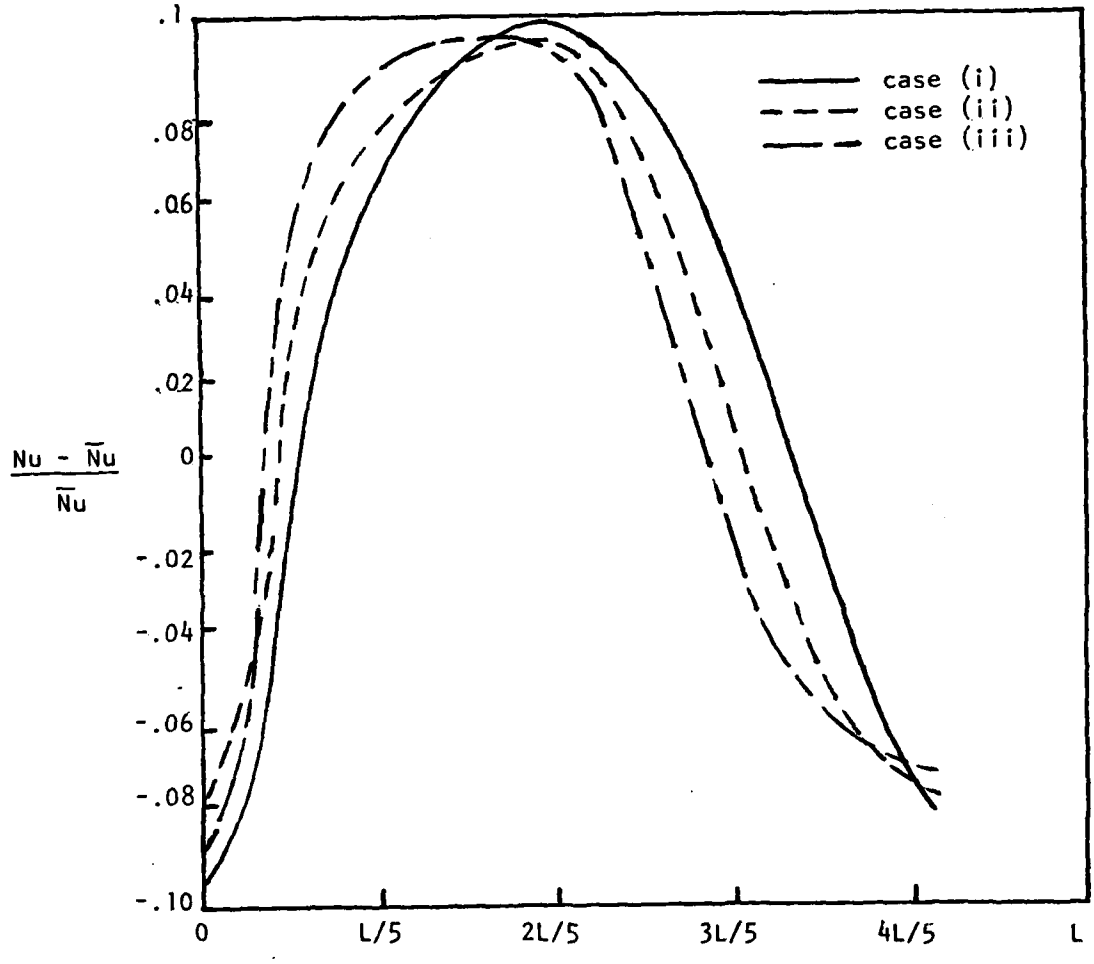

Figure 8. Longitudinal variation of the local Nusselt number for the three boundary conditions imposed at the open end.

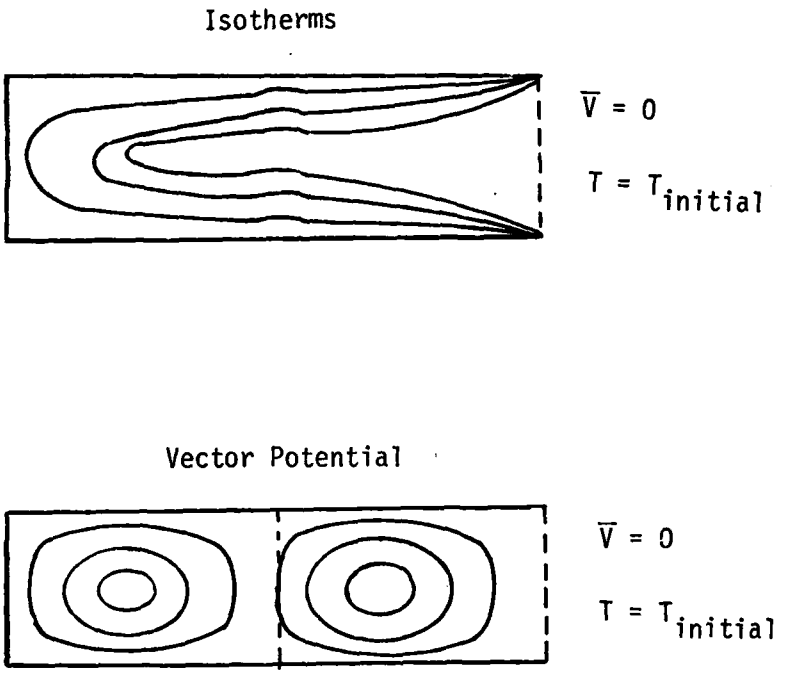

Figure 9. Longitudinal representation of isotherm and vector potential profiles.

evaluated at $\bar{T}_b$. Correlations of the type $Nu = CR_a^n$ are presented in Table 1 for various geometries and boundary conditions found in the literature.

These type of correlations tend to smooth out the boundary conditions imposed as well as the system geometry. The present study results are given in the table for n = .25 where the length scale is chosen to be the cylinder diameter (entree 6). For comparison with Maas [8], the uniform heat flux case, a .21 power was forced with the resulting value of C = 1.81 which is 49% higher than that found by Maas. Changing the length scale, L, in evaluating Nu and Ra to represent three dimensional effects such that

$$\frac{1}{L} = \frac{1}{L_H} \frac{1}{L_D}$$

where L_H is the horizontal axial length and L_D the diameter yields the result of entree 8 in the table. Although this is closer to the correlations of Maas and Deaver and Eckert higher values of Nu, for the same Ra are calculated. This is suspected to be a result of the end boundary effects - the additional induced buoyancy in the flow which is shown in Figure 9 may enhance the heat transfer rates, compared to the two dimensional case.

Representative values for the natural convective film coefficient were incorporated into an existing finite element radiation model to determine wall temperature values. This was carried out at the Arnold Air Station, TN and applied to a specific test facility. To date, experimental verification of the results have not been complete. The analysis indicates an approximate ten percent increase in the overall wall heat transfer rate due to natural convection.

TABLE 1. Comparison of Mean Nusselt Number Correlations

Investigator*	n	C	Condition
1. Deaver & Eckert [7]	.214	1.181	Experiment, increasing wall temperature
2. Maas [8]	.210	1.215	Experimental, uniform wall heat flux
3. Evans & Stefany [9]	.25	0.55	Experimental, step change in wall temperature
4. Kuehn & Goldstein [10]	.25	0.20	Experimental, annulus
5. Ozoe, Sayama and Churchill [11]	.336	.0981	Experimental, rectangular channel, aspect ratio = 1
6. Present Study	.25	1.13	Numerical, three dimensional
7. Present Study	.210	1.81	Numerical, three dimensional
8. Present Study	.210	1.61	Length scale = $\frac{1}{L_H} + \frac{1}{L_R}$

*Sources are listed in Reference section

RECOMMENDATIONS FOR FURTHER STUDIES

The numerical model developed in this project was applied to a specific configuration (a fixed length-to-diameter ratio) and boundary conditions (constant wall heat flux). Only a limited range of Ra was investigated to be consistent with the Arnold Air Station test facility conditions. Only slight variations in axial heat flux was found, compared to two dimensional models.

If larger values of Ra are to be imposed, which may be the case for very high gas temperatures or if using a high Prandtl number fluid a transition to turbulent conditions will result. It is recommended that in order to study this problem the numerical model be generated in two dimensions (r and ϕ) so that a much finer grid space can be used. Turbulence modelling should then be introduced, such as a simple algebraic stress formulation or a more rigorous turbulent transport analysis such as has been applied to external buoyant shear flows by Liburdy, Groff and Faeth [5] and Liburdy and Faeth [6].

In addition, in order to test these models, it is necessary to carry out experimental verifications. These studies should be capable of measuring surface heat flux rates, bulk fluid temperatures, and velocity and temperature profiles. In addition, for extension into the turbulent regime, fluctuating temperature and velocity components, and appropriate cross correlations as possible should be measured. Only a limited number of such studies have been performed in natural convecting flow in enclosures in general. The instrumentation must be rather sophisticated in order not to

interrupt the flow field (laser velocimeter techniques seem most appropriate for velocity measurements and fine wire thermocouples for temperature data have been used previously to yield satisfactory results).

PUBLICATIONS AND PAPER PRESENTATIONS

Some of the information contained in this report which has resulted from U.S.A.F. Contract F49620-79-C-0168 has been presented at the Southeastern Thermal Science Seminar, Florida Atlantic University, Boca Raton, Florida, May, 1979 and appears in the Abstracts of that meeting.

Further modifications to the computational scheme in future studies as well as matching experimental data is anticipated as discussed in the section on Recommendations for Further Study. Such future investigations are expected to add to the rather limited archival knowledge of turbulent natural convection in enclosures.

ASSOCIATED PERSONNEL

One graduate assistant, Mr. Parm-Pal Singh, assisted with the computational efforts of this study. Mr. Singh is a Ph.D. candidate in the Mechanical Engineering Department at Clemson University under the thesis advisorship of James A. Liburdy (principal investigator).

REFERENCES

1. Aziz, K. and Hellums, J. D., "Numerical Solution of the Three Dimensional Equations of Motion for Laminar Natural Convection," Physics of Fluids, V. 10, No. 2, 1967, pp 314-324.

2. McAdams, W. H., Heat Transmission, 3rd Ed., McGraw-Hill Book Co. Inc., New York, 1951.

3. Kee, R. J. and McKillop, A. A., "A Numerical Method for Predicting Natural Convection in Horizontal Cylinders with Asymmetric Boundary Conditions," Computers and Fluids, V. 5, 1977, pp 1-14.

4. Forsythe, G. E. and Watson, W. R., Finite-Difference Methods for Partial Differential Equations, John Wiley & Sons, Inc., New York, 1967.

5. Liburdy, J. A., Groff, E. G., and Faeth, G. M., "Structure of a Turbulent Thermal Plume Rising Along an Isothermal Wall," J. Heat Transfer, V. 101, No. 2, May 1979, pp 249-255.

6. Liburdy, J. A. and Faeth, G. M., "An Experimental Investigation of a Turbulent Plume Along an Isothermal Wall," Symposium on Turbulent Shear Flows, April 18-20, University Park, PA, 1977.

7. Deaver, F. K. and Eckert, E. R. G., "An Interferometric Investigation of Convective Heat Transfer in a Horizontal Fluid Cylinder with Wall Temperature Increasing at a Uniform Rate," Heat Transfer 1970, V. IV, Elsevier Pub. Co., Amsterdam, 1970.

8. Maas, H. G., "Transient Natural Convection Heat Transfer in a Horizontal Cylinder," Ph.D. Thesis, University Washington, 1964.

9. Evans, L. B. and Stefany, N. E., "An Experimental Study of Transient Heat Transfer to Liquids in Cylindrical Enclosures," Chem. Engineering Progress Symposium Series, No. 64, V. 62, 1967, pp 209-215.

10. Kuehn, T. K. and Goldstein, R. J., "An Experimental and Theoretical Study of Natural Convection in the Annulus Between Horizontal Concentric Cylinders," J. Fluid Mechanics, V. 74, Part 4, 1976, pp 695-719.

11. Ozoe, H., Sayama, H., Churchill, S. W., "Natural Convection in an Inclined Rectangular Channel at Various Aspect Ratios and Angles - Experimental Results," Int. J. Heat Mass Transfer, V. 18, 1975, pp 1425-1431.

Unclassified

SECURITY CLASSIFICATION OF THIS PAGE (When Data Entered)

REPORT DOCUMENTATION PAGE	READ INSTRUCTIONS BEFORE COMPLETING FORM
1. REPORT NUMBER (19) AFOSR-TR-80-0262 (18) / 2. GOVT ACCESSION NO.	3. RECIPIENT'S CATALOG NUMBER
4. TITLE (and Subtitle) (6) THREE-DIMENSIONAL TRANSIENT NATURAL CONVECTION IN A HORIZONTAL CYLINDER: A NUMERICAL ANALYSIS.	5. TYPE OF REPORT & PERIOD COVERED (9) FINAL rept. 16 May [redacted]-31 Dec [redacted]79 / 6. PERFORMING ORG. REPORT NUMBER
7. AUTHOR(s) (10) JAMES A. LIBURDY	8. CONTRACT OR GRANT NUMBER(s) (15) F49620-79-C-0168
9. PERFORMING ORGANIZATION NAME AND ADDRESS CLEMSON UNIVERSITY MECHANICAL ENGINEERING DEPT CLEMSON, SOUTH CAROLINA 29631	10. PROGRAM ELEMENT, PROJECT, TASK AREA & WORK UNIT NUMBERS (16) 2307/A4 61102F (17) A4
11. CONTROLLING OFFICE NAME AND ADDRESS AF OFFICE OF SCIENTIFIC RESEARCH/NA (11) BLDG 410 BOLLING AFB, DC 20332	12. REPORT DATE Feb [redacted]80 / 13. NUMBER OF PAGES 36
14. MONITORING AGENCY NAME & ADDRESS(if different from Controlling Office) (12) 39	15. SECURITY CLASS. (of this report) UNCLASSIFIED / 15a. DECLASSIFICATION/DOWNGRADING SCHEDULE

16. DISTRIBUTION STATEMENT (of this Report)

Approved for public release; distribution unlimited.

17. DISTRIBUTION STATEMENT (of the abstract entered in Block 20, if different from Report)

18. SUPPLEMENTARY NOTES

19. KEY WORDS (Continue on reverse side if necessary and identify by block number)

NATURAL CONVECTION
NUMERICAL MODELING

20. ABSTRACT (Continue on reverse side if necessary and identify by block number)

A mathematical formulation of the governing equations for transient natural convection in a finite length horizontal cylinder is developed and constructed in finite difference form. The boundary conditions consist of radial heat flux for a specified thermal resistance, axial heat flux from one closed end and three different conditions at the other end to represent exposure to a hot convecting gas environment. The formulation is expressed in terms of the vorticity equations, energy equation and a set of vector potential equations. Solution is by the alternating direction implicit method for the vorticity and →

DD FORM 1 JAN 73 1473 EDITION OF 1 NOV 65 IS OBSOLETE

UNCLASSIFIED 442697

SECURITY CLASSIFICATION OF THIS PAGE (When Data Entered)

energy equations and the successive over relaxation method for the vector potential equations. Numerical experiments were run using the model to determine the local wall heat flux and the local wall temperatures. Wall thermal resistance values and the aspect ratio (length-to-diameter) was chosen to be consistent with the Air Force test facility at AEDC. A heat transfer correlation is presented in terms of the Nusselt and Rayleigh numbers. Steady state conditions are obtained for the nondimensional time approximately equal to .005. Circumferential heat transfer coefficient variations are shown with larger values occurring near the top of the cylinder. Axial coefficients vary within approximately 10 percent with the largest values occurring near the center of the cylinder. With respect to test conditions at the AEDC facility, the convective components appear to be less than 10 percent of the radiative heat flux to the cylinder walls when a high temperature gas (air) is enclosed in the cylinder.